Brownian Motion Exhibiting Absolute Negative Mobility

Ralf Eichhorn, Peter Reimann, and Peter Hänggi

Universität Augsburg, Theoretische Physik I, Universitätsstrasse 1, D-86135 Augsburg, Germany

We consider a single Brownian particle in a spatially symmetric, periodic system far from thermal equilibrium. This setup can be readily realized experimentally. Upon application of an external static force F, the average particle velocity is negative for $F > 0$ and positive for $F < 0$ (absolute negative mobility).

When a system at rest is perturbed by a static force, we expect that it responds by moving in the direction of that force. The rather surprising opposite behavior in the form of a permanent motion against a (not too large) static force of whatever direction is called *absolute negative mobility* (ANM) [1,2]. If the unperturbed system is at thermal equilibrium, then ANM is impossible since it could be exploited to construct a *perpetuum mobile* of the second kind. Legendary but quite complex nonequilibrium systems which do exhibit ANM are "donkeys" [3]. In this Letter we demonstrate that even a simple, structureless Brownian particle can exhibit ANM away from thermal equilibrium in a setup which can easily be realized experimentally—a scenario hitherto commonly considered as impossible.

Going *in medias res,* let us consider the overdamped 2D Brownian motion,

$$\eta \dot{x}(t) = -\partial_x V[x(t), y(t)] + \xi_x(t), \tag{1}$$
$$\eta \dot{y}(t) = -\partial_y V[x(t), y(t)] + \xi_y(t) + F,$$

where η is the viscous friction coefficient and $V(x, y)$ is the hard-wall potential from Fig. 1a, confining the Brownian motion to a "corridor" along the y axis with *symmetric, periodic* obstacles. Further, $\xi_x(t)$ are thermal fluctuations, modeled by unbiased Gaussian white noise with $\langle \xi_x(t) \xi_x(s) \rangle = 2\eta k_B T \delta(t - s)$, where k_B denotes Boltzmann's constant and T the temperature. If $\xi_y(t)$ is an independent, second thermal white noise source, then (1) is an equilibrium system and the average particle current

$$\langle \dot{y} \rangle := \left\langle \lim_{t \to \infty} \frac{y(t) - y(t_0)}{t - t_0} \right\rangle \tag{2}$$

always runs into the direction of the static force F. Figure 1b depicts the corresponding $\langle \dot{y} \rangle$-F characteristics for the simplest nonequilibrium model, namely a *symmetric* dichotomous noise $\xi_y(t)$, with the promised ANM as its most outstanding feature.

Our first remark is that the so-called ratchet effect [4] is characterized by a current $\langle \dot{y} \rangle$ which is nonzero for $F = 0$ and does not change its direction within an entire neighborhood of $F = 0$. This effect thus inevitably involves some kind of asymmetry (for $F = 0$), whereas our present system is perfectly symmetric. Second, so-called *differential negative mobility* (or resistance) [5] is typified by a nega-

tive slope of the $\langle \dot{y} \rangle$-F characteristics *away* from $F = 0$. Thus, in both cases the salient feature of ANM is absent, namely a current $\langle \dot{y} \rangle$ which is always opposite to the (not too large) force F, independently of whether F is positive or negative. Finally, we mention that ANM has also been observed in semiconductor devices [1] and in models for coupled Brownian motors [2,3]. However, in the first case it has an entirely quantum mechanical origin, and in the second case it is a genuine collective effect, without leaving room for any kind of *classical, single-particle* counterpart. Accordingly, the respective physical mechanisms are completely different from ours.
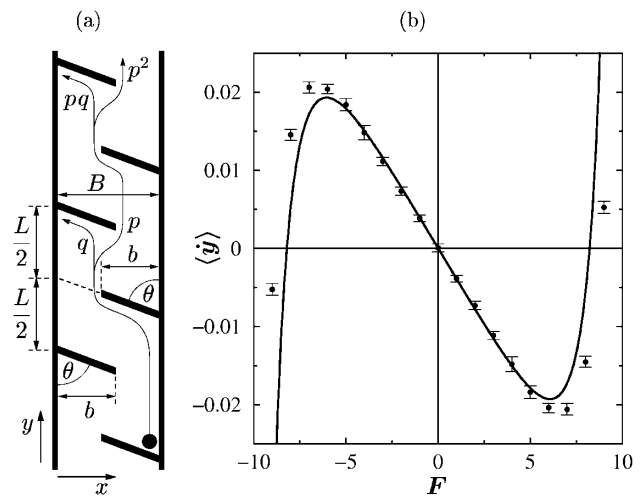

FIG. 1. (a) Hard-wall potential $V(x, y)$, defined as zero in the white and infinity in the black regions. It confines the motion of a particle to a "corridor" of width B along the y axis (the white regions outside this corridor are of no interest). The black obstacles are arranged in a symmetric, periodic manner (180° rotation symmetry) and are characterized by the parameters θ and b (their extension in the y direction is neglected). Note that $b > B/2$. Several typical traveling routes of a particle under the action of a static force $F_{\text{tot}} > 0$ along the y axis are indicated as arrows together with their probabilities ($q := 1 - p$). (b) The current (2) versus the static force F in (1) for the potential $V(x, y)$ from (a), Gaussian white noise $\xi_x(t)$, and a dichotomous noise $\xi_y(t)$ that flips at a rate γ between $\pm A$. Using dimensionless units, the parameter values are $\eta = 1$, $L = 1$, $B = 1$, $b = 0.55$, $\theta = 45°$, $k_B T = 0.1$, $A = 10$, $\gamma = 0.4$. Dots with error bars: numerical simulations of (1). Solid line: analytic approximation (3)–(5).

Returning to the ANM in Fig. 1b, its origin can be understood as follows: Consider a (moderately large) time interval τ during which the dichotomous noise $\xi_y(t)$ in (1) is constant and $F_{\text{tot}} := \xi_y(t) + F > 0$. When starting in one of the "corners" between the right "corridor wall" and any of the adjacent obstacles (see Fig. 1a), the particle first closely follows the right corridor wall until it hits the next obstacle, then "slides down the back" of that obstacle, and afterwards performs a "free fall" in the y direction. Since the lateral extension of the obstacles b exceeds half the corridor width $B/2$ the particle then hits with a high probability q the next obstacle on its way and ends up by being trapped in the corresponding (left) corner. In order to avoid this trap, the particle has to thermally diffuse at least over a distance $b - (B - b) = 2b - B$ in the positive x direction during its free fall in the y direction. With *increasing* force F_{tot}, the available time and therefore the probability $p := 1 - q$ of such a diffusive displacement decreases, implying that the particle travels on the average a *shorter* distance along the y axis during the time τ. Since an analogous consideration applies for time intervals τ with $F_{\text{tot}} = \xi_y(t) + F < 0$, the particle motion on the average acquires a bias in the direction opposite to the static force F; i.e., it exhibits ANM.

In order to quantify this argument, we first note that the above-mentioned probability p of avoiding a trap (for $F_{\text{tot}} > 0$) can be approximated as [6]

$$p(F_{\text{tot}}) = \frac{1}{2} - \frac{1}{2}\operatorname{erf}\left(\frac{2b - B}{\sqrt{2Lk_BT}}\sqrt{F_{\text{tot}}}\right), \qquad (3)$$

where $\operatorname{erf}(x) := 2\pi^{-1/2}\int_0^x e^{-y^2}\,dy$. With probability p, a particle thus covers in addition to the "basic distance" of approximately $3L/2$ another period L (see Fig. 1a). It then avoids the second trap on its way with approximately the same (relative) probability p as in (3), i.e., a second period L is covered with (absolute) probability p^2, etc.; see Fig. 1a. If the maximal traveling distance (avoiding all traps) is of the form $(3/2 + N)L$ with $N \in \mathbb{N}$, the average traveling distance $\Delta y(\tau, F_{\text{tot}})$ thus follows as $L[3/2 + p + p^2 + \cdots + p^N]$. Neglecting that the "free traveling speed" $v_y := F_{\text{tot}}/\eta$ is slightly reduced when the particle slides down the back of an obstacle, we obtain $(3/2 + N)L = v_y\tau$ and hence

$$\Delta y(\tau, F_{\text{tot}}) = L\left\{\frac{1}{2} + \frac{1 - [p(F_{\text{tot}})]^{\frac{F_{\text{tot}}\tau}{\eta L} - \frac{1}{2}}}{1 - p(F_{\text{tot}})}\right\}. \qquad (4)$$

This expression remains a decent interpolation even if $v_y\tau$ is not of the form $(3/2 + N)L$. Symmetrically, for $F_{\text{tot}} < 0$ the average traveling distance is $-\Delta y(\tau, -F_{\text{tot}})$, implying for the net average current (2) the approximation

$$\langle \dot{y} \rangle = \frac{\int_0^\infty d\tau\, \rho(\tau)\,[\Delta y(\tau, A + F) - \Delta y(\tau, A - F)]}{2\int_0^\infty d\tau\, \rho(\tau)\tau}, \qquad (5)$$

where $\pm A$ are the two states of the dichotomous noise $\xi_y(t)$ and $\rho(\tau) = \gamma e^{-\gamma\tau}$ is the distribution of sojourn times; i.e., γ is the flip rate.

The agreement of our analytic prediction (5) with the simulations in Fig. 1b is remarkably good in view of the various underlying approximations. In particular, our assumption that the particle covers at least a distance $3L/2$ during the time τ renders (4) doubtful unless $v_y\tau = F_{\text{tot}}\tau/\eta > 3L/2$. To fulfill this condition for all the forces $F_{\text{tot}} = A \pm F$ notably contributing in (5) requires that $A - |F| > 3\gamma\eta L/2$. Indeed, for $A < 3\gamma\eta L/2$ ANM is found to disappear in numerical simulations of (1).

On the other hand, ANM is expected to subsist for numerous generalizations of our original model (1). Figure 2 exemplifies a setup with a 2D array of obstacles. For symmetry reasons, the current (2) remains exactly the same as in Fig. 1, but the parallelization now admits to simultaneously transport a much larger number of particles. Such a device can be readily realized by a modification of those studied experimentally in [7] and theoretically in [8]. We emphasize that while these modifications of the experimental setups are straightforward, the physics, however, is completely different. A further step towards a realistic experimental system is achieved by choosing

$$\xi_y(t) = \xi_{\text{th}}(t) + f(t), \qquad (6)$$

where $\xi_{\text{th}}(t)$ is another thermal white noise like $\xi_x(t)$ (but statistically independent) and $f(t)$ switches *periodically* between $\pm A$ with $\rho(\tau) = \delta(\tau - \tau_{ac})$. For not too weak driving $f(t)$ and with the appropriately adjusted definition $F_{\text{tot}} := f(t) + F$, the corrections in (3) and (4) due to the thermal noise $\xi_{\text{th}}(t)$ are small, and thus (5) remains a valid approximation provided $A - |F| > 3\eta L/2\tau_{ac}$.

An experimental realization of the system (1) and (6) along the lines of [7,9] is presently under construction in the laboratories of Bechinger and Leiderer. Henceforth, we
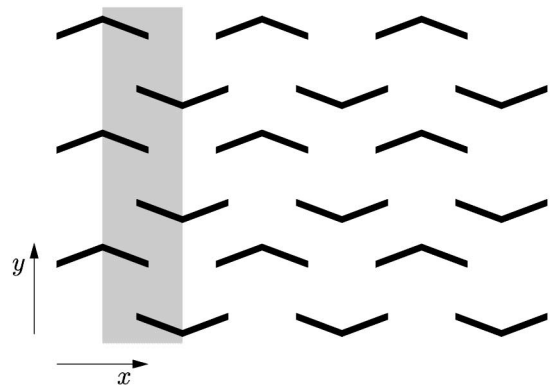
FIG. 2. Hard-wall potential $V(x, y)$ like in Fig. 1a but now periodically continued along the x axis, resulting in a 2D array of obstacles ("sieve"). For symmetry reasons, the y component of the Brownian motion (1) is completely independent of whether the grey shaded "corridor" is endowed with perfectly reflecting "sidewalls" (Fig. 1a) or not.
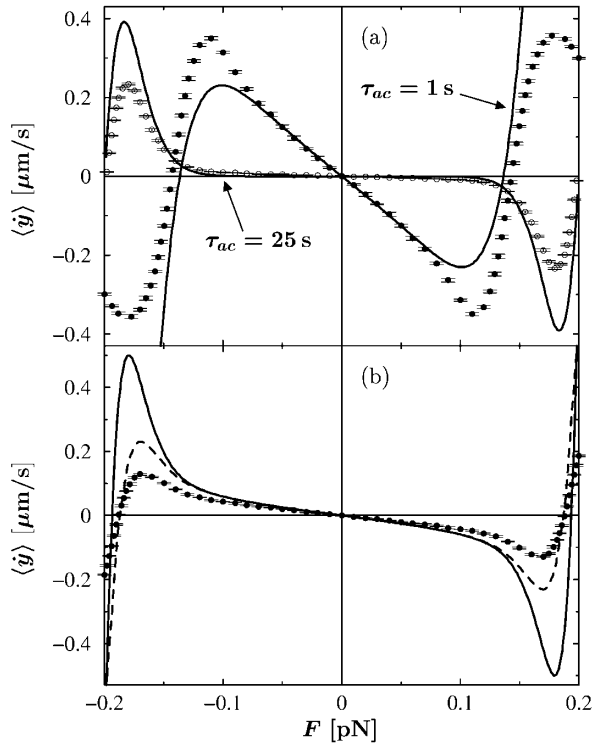
FIG. 3. The current (2) versus the static force F in (1) and (6) for the potential $V(x, y)$ from Fig. 1a or Fig. 2, independent Gaussian white noises $\xi_x(t)$ and $\xi_{th}(t)$, and a periodic driving $f(t)$ that jumps between $\pm A$ with time constant τ_{ac}. The parameter values are $L = 4\ \mu m$, $B = 3\ \mu m$, $b = 1.2\ \mu m$, $\theta = 70°$, $T = 293$ K, $A = 0.2$ pN. The Brownian particle is assumed as spherical with radius $r = 0.5\ \mu m$ and as subjected to Stokes friction $\eta = 6\pi\nu r$, where ν is the viscosity of water. Dots with error bars: numerical simulations of (1) and (6) with $\tau_{ac} = 1$ s and $\tau_{ac} = 25$ s in (a) and with $\tau_{ac} = 5$ s in (b). Solid line in (a) with $\tau_{ac} = 1$ s: Analytic approximation (3)–(5) with $\rho(\tau) = \delta(\tau - \tau_{ac})$. Solid line in (a) with $\tau_{ac} = 25$ s: Analytic approximation (3), (7)–(9) with $\tau = \tau_{ac}$. Solid line in (b): Analytic approximation by adding up (4) and (7) and then evaluating (5) with (3), (9), $\rho(\tau) = \delta(\tau - \tau_{ac})$, and $\tau_{ac} = 5$ s. Dashed line in (b): Analytic approximation for $\tau_{ac} = 5$ s based on (10) and (11), as described in more detail in the main text. Note that all analytical results are based on the assumption of a point particle. The finite particle radius r has been approximately accounted for by replacing B by $B - 2r$ in (3).

focus on such experimentally realistic parameter values in our quantitative examples; see Fig. 3. In particular, the agreement of (5) with the numerical simulations in Fig. 3a for $\tau_{ac} = 1$ s is again rather good in the parameter range $|F| < 0.14$ pN compatible with $A - |F| > 3\eta L/2\tau_{ac}$.

In (4), we have completely neglected the possibility that a trapped particle may escape from the trap due to the ambient thermal noise. This is justified as long as τ is much smaller than the mean escape time $\tau_{esc}(F_{tot})$ out of a trap. Turning to the opposite case $\tau \gg \tau_{esc}(F_{tot})$, we start by calculating the time which a particle needs to advance by one period L along the y axis for $F_{tot} > 0$: This time is approximately L/v_y if the trap within such a period is

avoided and $L/v_y + \tau_{esc}(F_{tot})$ otherwise. The respective probabilities are p and $1 - p$, approximated by (3); i.e., the average time to cover one period L is $pL/v_y + [1 - p][L/v_y + \tau_{esc}(F_{tot})]$. The resulting average traveling distance during the (large) time $\tau \gg \tau_{esc}(F_{tot})$ is

$$\Delta y(\tau, F_{tot}) = \frac{\tau L}{\frac{L\eta}{F_{tot}} + [1 - p(F_{tot})]\tau_{esc}(F_{tot})}. \qquad (7)$$

Thus, if those large τ dominate, $\Delta y/\tau$ becomes independent of τ and (5) can be rewritten as

$$\langle \dot{y} \rangle = \frac{1}{2}\left[\frac{\Delta y(\tau, A + F)}{\tau} - \frac{\Delta y(\tau, A - F)}{\tau}\right], \qquad (8)$$

independent of $\rho(\tau)$. For small $F_{tot} > 0$, the first term in the denominator of (7) dominates and hence Δy increases in the expected linear response manner with increasing F_{tot}. As F_{tot} gets larger, $1 - p$ approaches 1 [cf. (3)] and the escape time τ_{esc} increases very fast [cf. (9) below], implying the existence of a maximum and a subsequent decay of Δy. As a consequence of this increasing "stickiness" of the traps with increasing F_{tot} [1,5], we recover once again ANM in (8) provided A is sufficiently large.

Focusing on the model (1) and (6), one can approximate $\tau_{esc}(F_{tot})$ by the mean first passage time from $x = 0$ to $x = b/\sin\theta$ of the auxiliary 1D dynamics $\eta\dot{x}(t) = -F_{tot}\cos\theta + \xi_x(t)$ with a reflecting boundary at $x = 0$, reading [10]

$$\tau_{esc}(F_{tot}) = \frac{b^2\eta}{k_B T}\frac{e^\alpha - \alpha - 1}{\alpha^2 \sin^2\theta},$$
$$\alpha := bF_{tot}\cot\theta/k_B T. \qquad (9)$$

The agreement of (7)–(9) with the numerical simulations in Fig. 3a for $\tau_{ac} = 25$ s is quite satisfactory. In particular, the predicted ANM is indeed recovered.

We emphasize that the basic physical origins of ANM are completely different in the small- and large-τ regimes as quantified by (4), (5) and (7), (8), respectively: In the former case, escapes out of the traps are negligible, while transient "first-trapping events" after each jump of F_{tot} provide the crucial mechanism for ANM. In the latter case, these transients are negligible, while the "re-escape events" are now at the origin of ANM. This remarkable feature that two completely different physical mechanisms both support one and the same phenomenon, suggests that ANM will also be present in the so far disregarded intermediate-τ regime. Furthermore, on the basis of our previous physical insight, an immediate educated guess is to add up (4) and (7) and then evaluate (5). Both these predictions are nicely confirmed by Fig. 3b.

A more sophisticated analysis can again be based on our usual assumption that a particle always closely passes by the leftmost edge of any obstacle attached to the "right corridor wall" when $F_{tot} > 0$, as indicated in Fig. 1a. Consequently, the traveling times through any period L are governed by one and the same probability distribution

$\psi(t)$, independent of the particle's past (Markov property). Similarly as in (7), this distribution is approximately given by

$$\psi(t) = p\,\delta(t - \tau_1) + (1 - p)\Theta(t - \tau_1)\frac{e^{-(t-\tau_1)/\tau_{esc}}}{\tau_{esc}}, \tag{10}$$

where $\Theta(t)$ is the Heaviside function and $\tau_1 := L/v_y$. In this way, the original 2D problem can be approximately reduced to a 1D, unidirectional hopping process characterized by $\psi(t)$. Such processes have been analyzed in detail in the context of renewal theory [11]. Along these lines, we obtain for the Laplace transformed displacement $\Delta\tilde{y}(s, F_{tot}) := \int_0^\infty dt\, \Delta y(t, F_{tot})e^{-ts}$ the result

$$\Delta\tilde{y}(s, F_{tot}) = \frac{L}{s}\,\frac{\tilde{\psi}(s)}{1 - \tilde{\psi}(s)}\,\frac{e^{\tau_1 s} - 1}{\tau_1 s}, \tag{11}$$

where $\tilde{\psi}(s)$ is the Laplace transform of $\psi(t)$. While the first two factors on the right hand side of (11) are well known [11], the last factor accounts for the fact that the particle actually proceeds continuously rather than in discrete jumps of length L. Moreover, after the Laplace backtransformation of (11), a final transformation $\Delta y(\tau, F_{tot}) \mapsto \Delta y(\tau - 3L/2v_y, F_{tot}) + 3L/2$ is required since the basic distance $3L/2$, which the particle covers before encountering the first trap [see Fig. 1a and below (3)], is not yet taken into account by (11). For very small and large τ values one then recovers our previous results (4) and (7), respectively, while for more general τ values, a numerical evaluation of the Laplace backtransformation is necessary. A more detailed derivation of these analytical results will be presented elsewhere. A typical example is depicted in Fig. 3b, in good agreement with the numerical simulations.

In conclusion, we have demonstrated that a single, classical Brownian particle in a periodic, symmetric 2D potential landscape can exhibit the *prima facie* quite astonishing phenomenon of absolute negative mobility under suitable far from equilibrium conditions. In general, the effect is simultaneously supported by two completely different physical mechanisms and, in contrast to [1], is not restricted to adiabatically slow nonequilibrium perturbations. The phenomenon is moreover robust against modifications of the potential. It can occur in practically any potential landscape that provides "traps" with increasing "stickiness" as external force strengths increase. The setup discussed here is particularly suitable for an experimental realization along the lines of [7–9].

[1] T. J. Banys, I. V. Parshelyunas, and Y. K. Pozhela, Sov. Phys. Semicond. **5**, 1727 (1972); V. V. Pavlovich and E. M. Epstein, *ibid.* **10**, 1196 (1976); B. J. Keay *et al.,* Phys. Rev. Lett. **75**, 4102 (1995); R. Aguado and G. Platero, Phys. Rev. B **55**, 12 860 (1997); L. Hartmann, M. Grifoni, and P. Hänggi, Europhys. Lett. **38**, 497 (1997); I. Goychuk, E. Petrov, and V. May, Phys. Lett. A **238**, 59 (1998).

[2] P. Reimann, R. Kawai, C. Van den Broeck, and P. Hänggi, Europhys. Lett. **45**, 545 (1999); P. Reimann, C. Van den Broeck, and R. Kawai, Phys. Rev. E **60**, 6402 (1999); J. Buceta, J. M. Parrondo, C. Van den Broeck, and F. J. de la Rubia, *ibid.* **61**, 6287 (2000); S. E. Mangioni, R. R. Deza, and H. S. Wio, *ibid.* **63**, 041115 (2001).

[3] B. Cleuren and C. Van den Broeck, Europhys. Lett. **54**, 1 (2001).

[4] For reviews see P. Hänggi and R. Bartussek, Lect. Notes Phys. **467**, 294 (1996); R. D. Astumian and M. Bier, Biophys. J. **70**, 637 (1996); R. D. Astumian, Science **276**, 917 (1997); F. Jülicher, A. Ajdari, and J. Prost, Rev. Mod. Phys. **69**, 1269 (1997); P. Reimann, Phys. Rep. **361**, 57 (2002).

[5] S. R. White and M. Barma, J. Phys. A **17**, 2995 (1984); G. A. Griess and P. Serwer, Biopolymers **29**, 1863 (1990); V. Balakrishnan and C. Van den Broeck, Physica (Amsterdam) **217A**, 1 (1995); G. Cecchi and M. O. Magnasco, Phys. Rev. Lett. **76**, 1968 (1996); G. W. Slater, H. L. Guo, and G. I. Nixon, *ibid.* **78**, 1170 (1997).

[6] After drifting for a time t along the y axis with speed $v_y = F_{tot}/\eta$, the thermal diffusion along the x axis is approximately captured (for not too large t) by a Gaussian distribution with variance $\sigma^2 = 2Dt$. With Einstein's relation $D = k_B T/\eta$ and observing that neighboring obstacles have an overlap $2b - B$ (in the x direction) and an approximate distance $L/2$ (in the y direction) Eq. (3) follows.

[7] W. D. Volkmuth and R. H. Austin, Nature (London) **358**, 600 (1992); J. Rousselet, L. Salome, A. Ajdari, and J. Prost, *ibid.* **370**, 446 (1994); L. P. Faucheux and A. Libchaber, J. Chem. Soc. Faraday Trans. **91**, 3163 (1995); L. Gorre-Talini, J. P. Spatz, and P. Silberzan, Chaos **8**, 650 (1998); P. Serwer and G. A. Griess, J. Chromatogr. B **722**, 179 (1999); A. van Oudenaarden and S. G. Boxer, Science **285**, 1046 (1999); J. S. Bader *et al.,* Proc. Natl. Acad. Sci. U.S.A. **96**, 13 165 (1999).

[8] G. I. Nixon and G. W. Slater, Phys. Rev. E **53**, 4969 (1996); D. Ertas, Phys. Rev. Lett. **80**, 1548 (1998); T. A. J. Duke and R. H. Austin, *ibid.* **80**, 1552 (1998); I. Derényi and R. D. Astumian, Phys. Rev. E **58**, 7781 (1998).

[9] Q.-H. Wei, C. Bechinger, D. Rudhardt, and P. Leiderer, Phys. Rev. Lett. **81**, 2606 (1998); R. Bubeck, C. Bechinger, S. Neser, and P. Leiderer, *ibid.* **82**, 3364 (1999); C. Bechinger, M. Brunner, and P. Leiderer, *ibid.* **86**, 930 (2001).

[10] P. Hänggi, P. Talkner, and M. Borkovec, Rev. Mod. Phys. **62**, 251 (1990).

[11] D. R. Cox, *Renewal Theory* (Methuen & Co., London, 1962).